

# Spectral biases in tree-ring climate proxies

Jörg Franke<sup>1,2,3\*</sup>, David Frank<sup>1,3</sup>, Christoph C. Raible<sup>3,4</sup>, Jan Esper<sup>5</sup> and Stefan Brönnimann<sup>2,3</sup>

**External forcing and internal dynamics result in climate system variability ranging from sub-daily weather to multi-centennial trends and beyond<sup>1,2</sup>. State-of-the-art palaeoclimatic methods routinely use hydroclimatic proxies to reconstruct temperature (for example, refs 3,4), possibly blurring differences in the variability continuum of temperature and precipitation before the instrumental period. Here, we assess the spectral characteristics of temperature and precipitation fluctuations in observations, model simulations and proxy records across the globe. We find that whereas an ensemble of different general circulation models represents patterns captured in instrumental measurements, such as land-ocean contrasts and enhanced low-frequency tropical variability, the tree-ring-dominated proxy collection does not. The observed dominance of inter-annual precipitation fluctuations is not reflected in the annually resolved hydroclimatic proxy records. Likewise, temperature-sensitive proxies overestimate, on average, the ratio of low- to high-frequency variability. These spectral biases in the proxy records seem to propagate into multi-proxy climate reconstructions for which we observe an overestimation of low-frequency signals. Thus, a proper representation of the high- to low-frequency spectrum in proxy records is needed to reduce uncertainties in climate reconstruction efforts.**

Climate variability is driven on all timescales by external forcing and the internal dynamics of the system<sup>5</sup>. External forcings range from pulse-like events such as volcanic eruptions to changes on geologic timescales due to plate tectonics. Internal dynamics include rapid atmospheric processes as well as those arising from ocean convection and ice-sheet dynamics. The total variability can be divided into stochastic and periodic components ranging from the diurnal cycle to changes in Earth's orbit<sup>1</sup>.

Part of this variability continuum is fingerprinted in instrumental measurements spanning the past 100–250 years—a period that is additionally influenced by anthropogenic greenhouse-gas emissions. To assess pre-instrumental natural climate variability and changes over longer timescales, proxy records derived from tree rings, corals, lake sediments, ice cores, stalagmites or other archives<sup>4</sup> are necessary. Climate estimates derived from these archives contain a substantial fraction of noise (non-climate relevant information) and may contain mixed climatic signals (for example, precipitation and temperature<sup>6</sup>) of a poorly defined or even variable seasonality<sup>7</sup>. Temporal resolution can vary from seasonal to multi-centennial depending on the proxy type and can even change within one record. Variance artefacts may exist and thresholds might be reached (Supplementary Fig. S1). Data treatment required to extract the climate signals, for instance the removal of age-related trends in tree rings, has to be done carefully to avoid loss of low-frequency variability<sup>8</sup>. At the same

time, biological proxies may have enhanced low-frequency signals arising from lagged growth processes and responses<sup>9</sup>. These characteristics could influence the frequency spectra of proxy time series and might distort our understanding of high- to low-frequency climate variability.

To achieve a seamless quantification of climate in the past, present and future, the true variance across all frequency bands in the pre-industrial period needs to be properly captured. To determine whether this is the case, we estimate the variability continuum in instrumental observations<sup>10</sup>, the twentieth-century reanalysis<sup>11</sup> (20CR), multiple simulations for the past millennium<sup>12–15</sup> (GCM<sub>ens</sub>, Supplementary Section S3), annually resolved proxy records of at least 500 years in length (Supplementary Tables S1 and S2) and spatially resolved climate reconstructions<sup>16,17</sup>. The multi-centennial climate proxies are split into temperature- and precipitation-sensitive records by a correlation screening against annual mean instrumental temperature and precipitation<sup>10</sup> closely following the procedure applied in state-of-the-art climate reconstructions<sup>3</sup>. We exclude records if the interpretation of the proxy as temperature-/precipitation-sensitive made by the original authors does not agree with the correlation screening results. Fifty-six (128) temperature (precipitation) proxies, mainly tree-ring width (TRW) and tree-ring density (MXD), pass this screening. This collection of proxy records is representative for networks commonly aggregated in multi-proxy climate reconstructions of the late Holocene period<sup>3,16,17</sup>. We assess the continuum of variability by estimating the scaling exponent  $\beta$  of the spectral energy  $P(f) \propto f^{-\beta}$ , where  $f$  is the frequency that describes the continuum<sup>2</sup>. A  $\beta$ -value of zero corresponds to equal variability across all frequencies—a so-called white spectrum.  $\beta$ -values greater (smaller) than zero contain increased (reduced) low-frequency variance, and are referred to as red (blue) spectra.

Comparing instrumental, reanalysis and model spectra over the longest common frequency range (periods between 2 months and 100 years), we find close agreement in the representation of both temperature and precipitation spectra (Fig. 1). Temperature variability in the 20CR and GCM<sub>ens</sub> is characterized by a strong land–sea contrast<sup>18,19</sup> with higher  $\beta$ -values over the ocean (Fig. 1d,g; in both cases calculated for each simulation/ensemble member separately before averaging; see Methods). Decreasing  $\beta$ -values towards high latitudes<sup>2</sup> are clearly visible in Fig. 1a,d,g. Thermal inertia of the ocean plays an important role in the land–sea contrast<sup>2</sup>, whereas the latitudinal gradient is caused by low intra-annual variability in the tropical regions. These results are robust across various grid resolutions (Supplementary Fig. S4) as well as summer, winter and annual periods (Supplementary Fig. S5), indicating no seasonal dependence.

Similarly the precipitation data sets broadly agree in their spectral characteristics (Fig. 1b,e,h). However, relative to

<sup>1</sup>Swiss Federal Research Institute WSL, 8903 Birmensdorf, Switzerland, <sup>2</sup>Institute of Geography, University of Bern, 3012 Bern, Switzerland, <sup>3</sup>Oeschger Centre for Climate Change Research, 3012 Bern, Switzerland, <sup>4</sup>Physics Institute, University of Bern, 3012 Bern, Switzerland, <sup>5</sup>Department of Geography, Johannes Gutenberg University, 55099 Mainz, Germany. \*e-mail: franke@giub.unibe.ch.

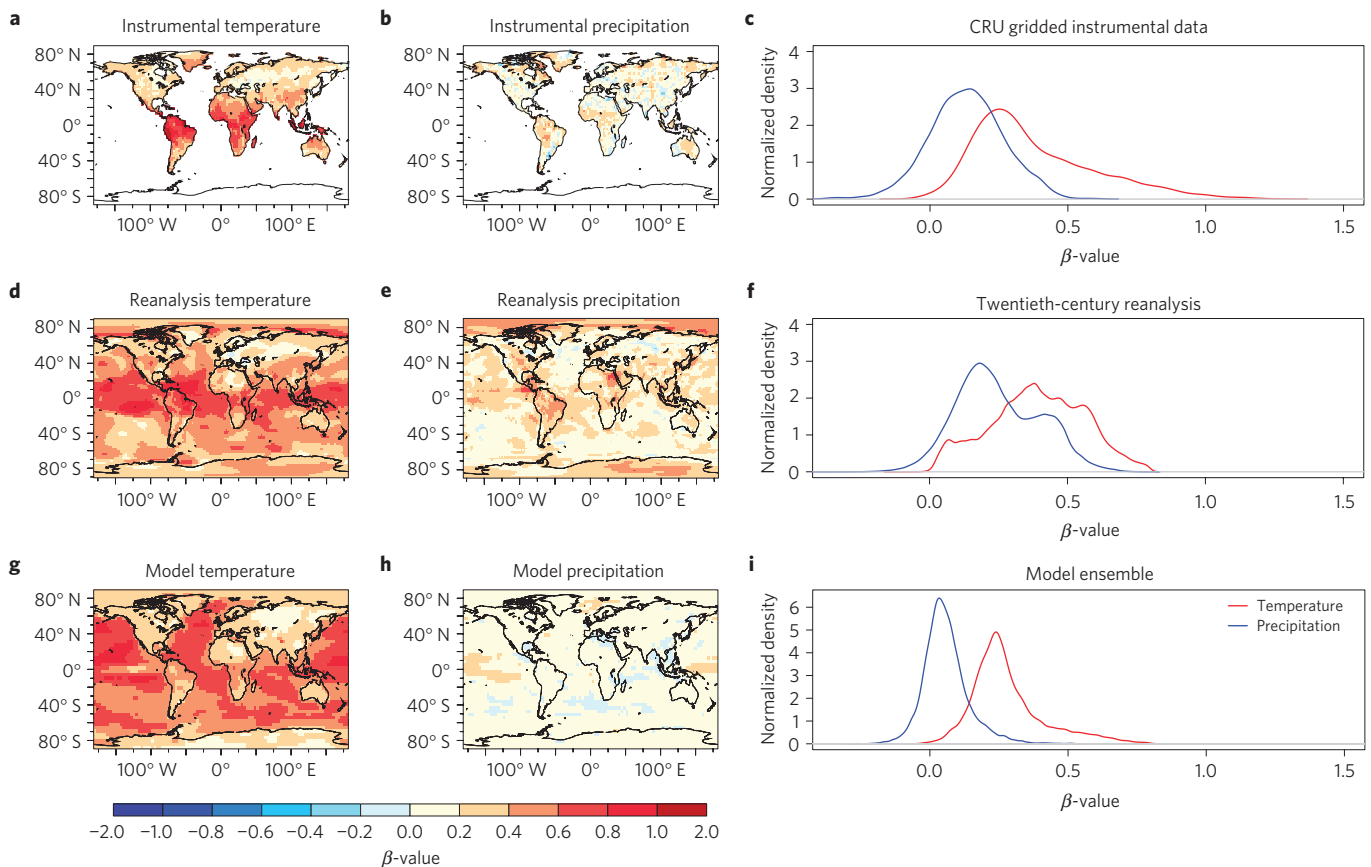


**Figure 1 | Spectral colour maps and distributions.** **a–c**, Spectral colour expressed as  $\beta$ -value for the gridded CRU TS3 temperature and precipitation data set (**a,b**), and the distributions of land-alone  $\beta$ -values (**c**; standardized; Gaussian smoothing kernel). **d–i**, The same as in **a–c** for the twentieth-century reanalysis data sets (**d–f**) and for the multi-model mean of each simulation's  $\beta$ -value field (**g–i**). All  $\beta$ -values are calculated for periods between 2 months and 100 years.

instrumental data, 20CR is slightly redder and the  $GCM_{ens}$  are slightly whiter. The state-of-the-art models used in this study have largely overcome previous criticisms related to prescribed flux corrections, challenges in modelling climate modes (for example El Niño/Southern Oscillation, Atlantic Multidecadal Oscillation) or missing forcings<sup>20,21</sup>, yet they may still not faithfully capture all multi-decadal to centennial climate variability. Small differences in the spatial patterns should furthermore be interpreted with caution as many regions lack high-quality precipitation observations. These discrepancies are all in line with the greater challenges in understanding hydro-climatic variability<sup>22</sup>. The generally low  $\beta$ -values (medians ranging from 0.05 in  $GCM_{ens}$  to 0.23 in 20CR) as well as the absence of a land–ocean contrast due to the reduced influences of thermal inertia are robust features of the precipitation spectra.

Most notably, we find clear differences between the temperature and precipitation spectra, with temperature variability from all data sources showing greater low-frequency loadings than precipitation. Globally aggregated, land-alone  $\beta$ -values of the instrumental data sets, 20CR and the  $GCM_{ens}$  are statistically distinguishable (Fig. 1c,f,i; two-sided Wilcoxon test, for all cases  $p < 0.001$ ). This conclusion is robust for varying frequency ranges, although the uncertainty for the individual  $\beta$ -values increases when shortening the frequency range (Supplementary Figs S6–S9).

Given the coherent picture of the climate system's variability continuum based on observations, reanalysis and model simulations, we test how well the proxy spectra match these estimates. Owing to the annual resolution of the proxy data considered, we

calculate  $\beta$ -values between periods of 2 years and 100 years. To robustly assess  $\beta$ -values across this frequency range, we perform additional analysis for early instrumental measurements of at least 200 years in length from central Europe<sup>23,24</sup> and the model data extracted for the same region and time period. This data subset yields similar results to those observed globally in Fig. 1, including distinct  $\beta$ -value distributions for temperature and precipitation (Fig. 2c,f). The global compilation of proxy data, in contrast, do not have the expected and distinguishable temperature and precipitation  $\beta$ -value distributions (Fig. 2i). Both distributions have a larger spread and are shifted towards significantly higher  $\beta$ -values, indicative of an overestimation of low-frequency variability in comparison with both observations and model simulations (Fig. 2f,g). Expected relationships between the proxy spectral characteristics and their geographic locations were not found (Supplementary Fig. S10c,d). Furthermore, spatially proximal proxies often differ substantially in their  $\beta$ -values even if derived from the same type of archive. Overall, we find that the proxy network poorly represents the expected characteristics of the climate system in the frequency domain.

Multiple factors may contribute to systematic spectral biases of proxies. Precipitation-sensitive proxies might respond to drought, that is a combination of precipitation, soil moisture and temperature-driven evapotranspiration. It is not obvious what spectrum a proxy that combines precipitation and temperature information will or should have. The  $\beta$ -values for drought records are mostly found in between those for precipitation and temperature (Supplementary Fig. S12). Yet

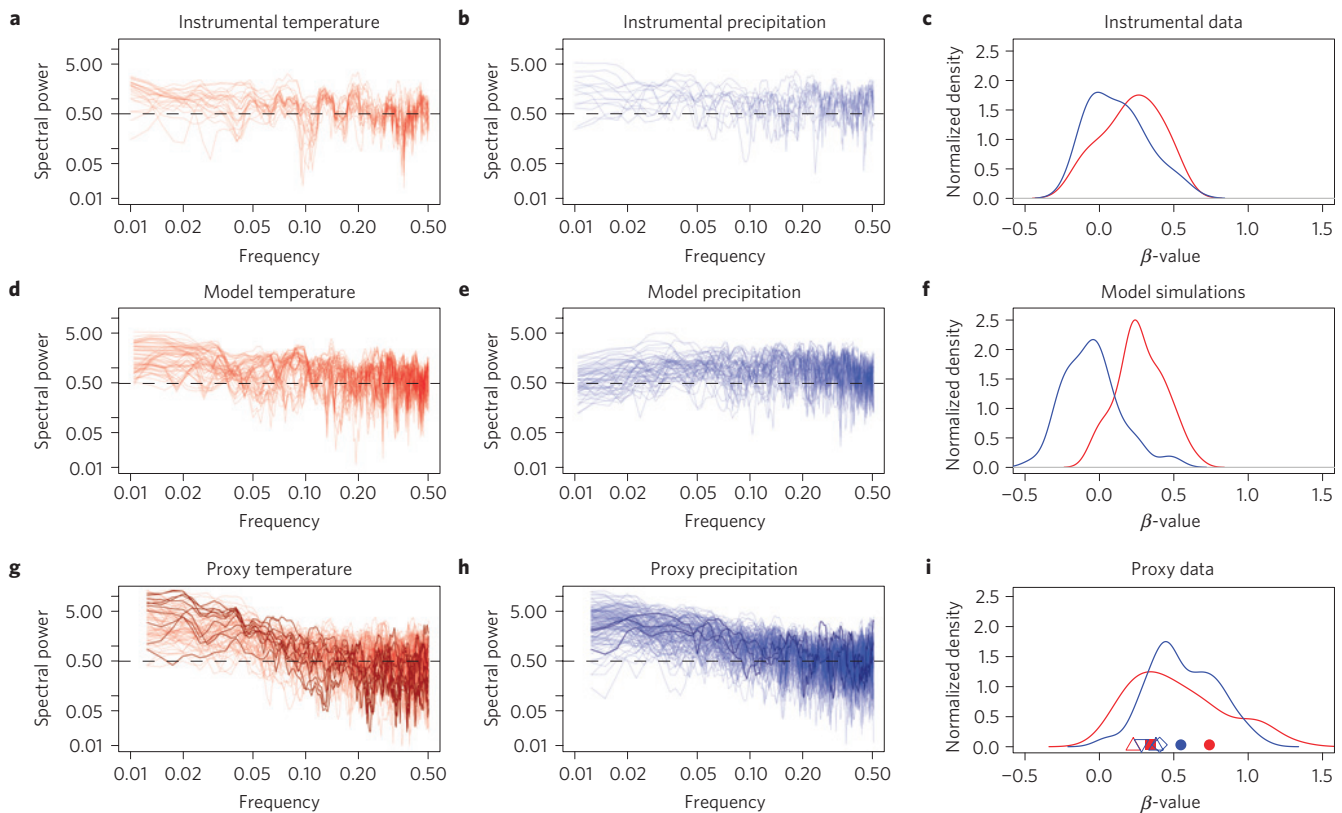


**Figure 2 | Long instrumental, GCM and proxy spectra.** **a–c**, Spectra of instrumental temperature (red; **a**), instrumental precipitation (blue; **b**) and associated  $\beta$ -value distributions from measurement series at least 200 years in length to allow 2–100-year spectral characterizations (**c**). **d–f**, As above but for GCM models at the instrumental locations. **g–i**, As above for global proxy data (light shades) and the European subset (dark shades). In **i**, median values for the different proxy archives are indicated as a square, MXD; circles, TRW; a diamond, tree-ring  $\delta^{18}\text{O}$ ; triangles, ice-core  $\delta^{18}\text{O}$ ; and a downtriangle, documentary data; with filled symbols for the median from  $n > 20$  and open symbols for  $n < 3$ .

there might be climatic regimes that would lead to red-biased spectra such as when precipitation and temperature are anticorrelated at inter-annual timescales but correlated at multi-decadal scales.

Furthermore, there is no reason to suspect that the diverse biological, chemical, physical, interpretational or analytical processes that characterize the formation and extraction of proxy climate information are the same for all proxy records (proxy type medians in Fig. 2i). Owing to the prevalence of tree-ring proxies in our data sets, we could test the spectral characteristics associated with the different types of proxy archive only for TRW and MXD temperature proxies (Supplementary Fig. S11). The TRW records generally fall towards the upper end of the proxy  $\beta$ -distribution, suggesting strong red biases (median  $\beta$  of 0.73), whereas the MXD records fall towards the lower end of the range expected for temperature (median  $\beta$  of 0.34). Biological proxies such as tree rings can integrate climate conditions over more than one year<sup>9</sup>, providing a mechanistic explanation for the red bias in TRW. Mechanistic understanding of the MXD parameter is less advanced, but given the necessary removal of age-related trends, the proper representation of high- and low-frequency variability remains a challenge in all types of tree-ring archive. These differences between the TRW and MXD data suggest that each proxy archive and parameter may have their own spectral biases and/or abilities to faithfully record the continuum of climate variability. Given that TRW records are the most commonly used proxy archive for late Holocene climate reconstructions<sup>3,4</sup>, our findings seem relevant for much of our understanding of the pre-industrial to industrial transition period. As additional proxy

archives (for example, speleothems, corals, ice cores, documentary data) play an increasingly dominant role in newer climate reconstructions their spectra will similarly require assessment of their spectral fidelity.

The spectral characteristics of climate proxies may be further modified by multi-proxy reconstruction techniques for a couple of reasons. First, the temporal evolution reconstructed for a particular location is a linear combination of multiple proxies. Second, on the basis of pseudo-proxy experiments<sup>25,26</sup>, reconstruction methods tend to cause a blue bias because they underestimate low-frequency variability. To investigate the extent to which biases in proxies may extend into multi-proxy compilations, we calculated  $\beta$ -values for annually resolved, proxy-based climate-field reconstructions of temperature<sup>17</sup> and precipitation<sup>16</sup>. The precipitation reconstruction has on average a whiter spectrum than the temperature reconstruction. Compared with observations, however, reconstructions for both variables (Fig. 3) are biased red, which suggests the propagation of the proxy bias into reconstructions. Similar evidence exists for other climate field reconstructions (Supplementary Fig. S13). More generally, the red bias of precipitation records and their use in temperature reconstructions<sup>3</sup> is worrying owing to the possibility that low-frequency proxy noise is responsible for spectral similarities<sup>27</sup>. These findings suggest that the understanding of high- to low-frequency temperature variability over the past millennium may be more limited than is widely assumed.

Our study gives evidence that attention to the spectral characteristics of the original proxy time series is needed. Proxies suffering from doubtful low-frequency signals, low quality, a

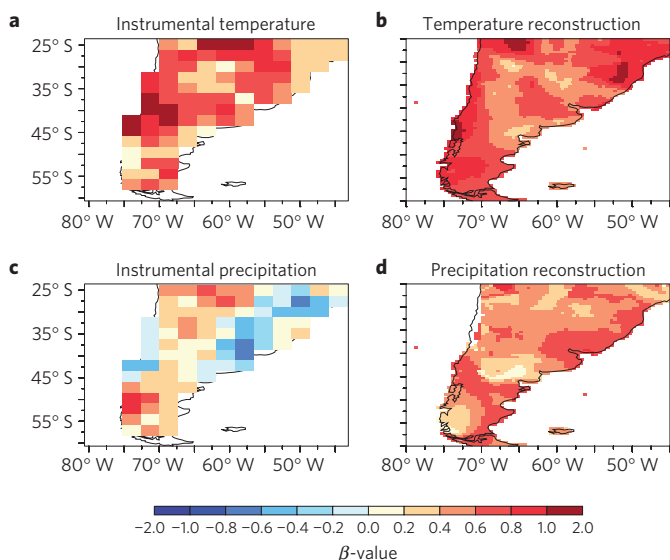


**Figure 3 | Spectral colour of climate reconstructions.** **a, b**, Mean spectral colour of the CRU TS3 temperature data set (**a**) and the annually resolved southern South American temperature reconstruction of ref. 17 (**b**). **c, d**, The same, for the CRU TS3 precipitation data set (**c**) and the precipitation reconstruction of ref. 16 (**d**). Both examples suggest that the spectral bias identified in proxy records propagates into climate reconstructions.

poor mechanistic understanding and further uncertainties such as variance or resolution changes over time, thresholds or gaps should be treated with caution. Precipitation-sensitive proxies should not be used in temperature reconstructions, nor vice versa, because of expected differences in their low-frequency variability<sup>28</sup>. Climate reconstructions using forward models in data assimilation approaches<sup>29</sup> offer a promising approach for handling mixed signals of different climate variables in proxies. In any case, reduced focus on the quantity of proxy records and increased focus on the quality is expected to facilitate an improved and seamless understanding of pre-anthropogenic to future climate variability.

## Methods

We compiled a global network of proxy archives, an ensemble of GCM simulations and instrumental measurements fully representative of data sets used to understand past, present and future climate. Climate time series were transformed into anomalies to exclude the annual cycle, and then linearly detrended and standardized (mean of zero and a standard deviation of one). Thomson's multitaper method was applied with three windows to transform records from the time to the frequency domain<sup>30</sup>. To evaluate the spectral continuum, we followed methods established in ref. 2. We calculated the so-called  $\beta$ -values as a measure of spectral colour by fitting a function through the spectrum. This function can be described with a power law:  $P(f) \propto f^{-\beta}$ , where  $P$  is the spectral energy,  $f$  is the frequency and  $\beta$  is the power-law exponent. Consequently, positive (negative)  $\beta$ -values indicate red (blue) spectra and a zero value a white spectrum. The slope of a linear least-squares fit between the log-frequency and log-power-density estimates represents the  $\beta$ -value estimates. We binned and averaged the spectra into equally spaced log-frequency intervals before the least-squares fitting to prevent overweighting of high-frequency variability.

For the model simulations and the twentieth-century reanalysis maps of  $\beta$ -values (Fig. 1), we calculated  $\beta$  for each individual simulation/ensemble member. Then, all ensemble members of a model were averaged to a model mean. Finally, all models were averaged to weight them equally independent of the number of available simulations.

Annually resolved, multi-centennial proxies were split into temperature- and precipitation-sensitive records by a two-step screening procedure: a state-of-the-art correlation screening<sup>3</sup> was applied to select records that correlate significantly (one-sided  $p < 0.1$  significance threshold) with annual mean instrumental temperature/precipitation (see Supplementary Section S11) of the corresponding

grid cell in the CRU TS3 data set<sup>10</sup>. Owing to first-order autocorrelation in many proxy records we used an effective sample size:

$$\text{Sample size}_{\text{effective}} = \text{Sample size} \frac{(1 - \text{first order autocorr. coeff.})}{(1 + \text{first order autocorr. coeff.})}$$

The resulting reduced degrees of freedom are used in the calculation of the significance threshold. We verified whether the proxy records are interpreted as temperature/precipitation-sensitive by the authors of the corresponding publication. Data derived from the International Tree-Ring Data Base, without direct associations to published process-based understanding of the climatic sensitivity, were screened only for correlation as trees can respond to both temperature and precipitation depending on the site environment.

Received 14 December 2011; accepted 7 January 2013;  
published online 3 February 2013

## References

- Ghil, M. in *Encyclopedia of Global Environmental Change* Vol. 1 (eds MacCracken, M. C. *et al.*) 544–549 (Wiley, 2001).
- Huybers, P. & Curry, W. Links between annual, Milankovitch and continuum temperature variability. *Nature* **441**, 329–332 (2006).
- Mann, M. E. *et al.* Global signatures and dynamical origins of the Little Ice Age and Medieval Climate Anomaly. *Science* **326**, 1256–1260 (2009).
- Jones, P. D. *et al.* High-resolution palaeoclimatology of the last millennium: A review of current status and future prospects. *Holocene* **19**, 3–49 (2009).
- Mitchell, J. An overview of climatic variability and its causal mechanisms. *Quat. Res.* **6**, 481–493 (1976).
- Büntgen, U. *et al.* Growth/climate response shift in a long subalpine spruce chronology. *Trees* **20**, 99–110 (2006).
- Frank, D. *et al.* A noodle, hockey stick, and spaghetti plate: A perspective on high-resolution paleoclimatology. *Wires Clim. Change* **1**, 507–516 (2010).
- Esper, J., Cook, E. R. & Schweingruber, F. H. Low-frequency signals in long tree-ring chronologies for reconstructing past temperature variability. *Science* **295**, 2250–2253 (2002).
- Frank, D. *et al.* Warmer early instrumental measurements versus colder reconstructed temperatures: shooting at a moving target. *Quat. Sci. Rev.* **26**, 3298–3310 (2007).
- Mitchell, T. D. & Jones, P. D. An improved method of constructing a database of monthly climate observations and associated high-resolution grids. *Int. J. Climatol.* **25**, 693–712 (2005).
- Compo, G. P. *et al.* The twentieth century reanalysis project. *Q. J. R. Meteorol. Soc.* **137**, 1–28 (2011).
- González-Rouco, J. F. *et al.* in *Solar Variability as an Input to the Earth's Environment* (ed. Wilson, A.) 329–338 (ESA Publications Division, 2003).
- Tett, S. F. B. *et al.* The impact of natural and anthropogenic forcings on climate and hydrology since 1550. *Clim. Dynam.* **28**, 3–34 (2007).
- Hofer, D., Raible, C. C. & Stocker, T. F. Variations of the Atlantic meridional overturning circulation in control and transient simulations of the last millennium. *Clim. Past* **7**, 133–150 (2011).
- Jungclauss, J. H. *et al.* Climate and carbon-cycle variability over the last millennium. *Clim. Past* **6**, 1009–1044 (2010).
- Neukom, R. *et al.* Multi-centennial summer and winter precipitation variability in southern South America. *Geophys. Res. Lett.* **37**, L14708 (2010).
- Neukom, R. *et al.* Multiproxy summer and winter surface air temperature field reconstructions for southern South America covering the past centuries. *Clim. Dynam.* **37**, 35–51 (2011).
- Pelletier, J. D. The power spectral density of atmospheric temperature from time scales of  $10^{-2}$  to  $10^6$  yr. *Earth Planet. Sci. Lett.* **158**, 157–164 (1998).
- Fraedrich, K. & Blender, R. Scaling of atmosphere and ocean temperature correlations in observations and climate models. *Phys. Rev. Lett.* **90**, 108501 (2003).
- Barnett, T. P. *et al.* Estimates of low frequency natural variability in near-surface air temperature. *Holocene* **6**, 255–263 (1996).
- Collins, M. *et al.* A comparison of the variability of a climate model with paleotemperature estimates from a network of tree-ring densities. *J. Clim.* **15**, 1497–1515 (2002).
- Schiermeier, Q. The real holes in climate science. *Nature* **463**, 284–287 (2010).
- Vose, R. S. *et al.* Global historical climatology network, 1753–1990. (Oak Ridge National Laboratory, 1998); available at <http://www.daac.ornl.gov>.
- Böhm, R. *et al.* The early instrumental bias: A solution for long central European temperature series 1760–2007. *Climatic Change* **101**, 41–67 (2010).
- Osborn, T. J. & Briffa, K. R. Climate: The real color of climate change? *Science* **306**, 621–622 (2004).

26. Von Storch, H. *et al.* Assessment of three temperature reconstruction methods in the virtual reality of a climate simulation. *Int. J. Earth Sci.* **98**, 67–82 (2009).
27. Moberg, A. *et al.* Analysis of the Moberg *et al.* (2005) hemispheric temperature reconstruction. *Clim. Dynam.* **31**, 957–971 (2008).
28. Casty, C. *et al.* A European pattern climatology 1766–2000. *Clim. Dynam.* **29**, 791–805 (2007).
29. Bhend, J. *et al.* An ensemble-based approach to climate reconstructions. *Clim. Past* **8**, 963–976 (2012).
30. Percival, D. & Walden, A. *Spectral Analysis for Physical Applications* (Cambridge Univ. Press, 1993).

### Acknowledgements

This study was financially supported by the EU project MILLENNIUM (#017008-GOCE) and by the Swiss National Science Foundation (SNSF) through its National Center of Competence in Research on Climate (NCCR Climate). C.R. and S.B. are also

supported by the Synergia project FUPSOL, and C.R. additionally by the EU project Past4Future. We thank NOAA/DOE/OBER for providing 20CR and everyone else who contributed model or proxy data for this study. We thank E. Gleeson for her editing efforts.

### Author contributions

J.E., J.F. and D.F. designed the study. J.F. performed the analysis with input from D.F., C.C.R. and S.B. All authors contributed to the discussion and to writing the paper.

### Additional information

Supplementary information is available in the [online version of the paper](#). Reprints and permissions information is available online at [www.nature.com/reprints](http://www.nature.com/reprints). Correspondence and requests for materials should be addressed to J.F.

### Competing financial interests

The authors declare no competing financial interests.